Salicylaldimine-Based Metal−Organic Framework Enabling Highly Active Olefin Hydrogenation with Iron and Cobalt Catalysts

Kuntal Manna,[†] Teng Zhang,[†] Michaël Carboni,[†] Carter W. Abney, and Wenbin Lin*

Department of Chemistry, University of Chicago, 929 East 57th Street, Chicago, Illinois 60637, United States

S *Supporting Information*

ABSTRACT: A robust and porous Zr metal−organic framework, sal-MOF, of UiO topology was synthesized using a salicylaldimine (sal)-derived dicarboxylate bridging ligand. Postsynthetic metalation of sal-MOF with iron(II) or cobalt(II) chloride followed by treatment with NaBEt$_3$H in THF resulted in Fe- and Co-functionalized MOFs (sal-M-MOF, M = Fe, Co) which are highly active solid catalysts for alkene hydrogenation. Impressively, sal-Fe-MOF displayed very high turnover numbers of up to 145000 and was recycled and reused more than 15 times. This work highlights the unique opportunity of developing MOF-based earth-abundant catalysts for sustainable chemical synthesis.

Although precious-metal complexes dominate the homogeneous catalysis literature, few of them have found industrial applications owing to their high price and inherent toxicity.[1] The replacement of precious metals with earth-abundant and less toxic elements, i.e., base metals, is thus at the forefront of contemporary molecular catalysis.[2−9] Homogeneous catalysts containing base metals are, however, prone to deactivation via intermolecular pathways. Steric protection around the metal centers by elaborately designed, sterically hindered ligands is a common strategy for designing stable catalysts, often at the expense of catalytic activities. Immobilization of homogeneous catalysts in structurally regular porous solid supports can provide catalytic site isolation without relying on bulky ligands, thus offering an alternative route to obtaining highly active base metal catalysts. Herein we report the first use of a metal−organic framework (MOF) for immobilizing highly active Fe(II)− and Co(II)−salicylaldimine catalysts for hydrogenation of alkenes.

Hydrogenation of olefins is one of the most important reactions in organic synthesis, though many industrially important hydrogenation reactions still rely on precious-metal catalysts.[10] Significant efforts have in recent years been devoted to discovering earth-abundant metal catalysts[5,11−19] most of which have limited lifetimes and modest activities. Parallel efforts have been devoted to the development of zeolite- and silica-supported iron- and cobalt-based heterogeneous hydrogenation catalysts,[20,21] bare or protected metallic nanoparticles,[22−28] or iron oxide nanoparticle-based catalysts.[29] However, the activities and lifetimes of these heterogeneous hydrogenation catalysts are still far from satisfactory.

As a new class of porous molecular materials, MOFs have attracted increasing interest in recent years owing to their potential applications in many areas, including gas storage,

separation, chemical sensing, drug delivery, and catalysis.[30−39] In particular, MOFs have provided an interesting platform for engineering single-site solid catalysts for various organic transformations.[40−44] The pores and channels in MOFs serve as confined spaces for the attachment or encapsulation of molecular catalysts, providing catalytic site isolation and thus preventing bimolecular catalyst deactivation.[45,46] Incorporation of orthogonal secondary functional groups into MOF backbones allows the convenient generation of different metal complexes, enabling the screening and discovery of novel molecular catalysts. In this work, a MOF containing an orthogonal salicylaldimine (sal) moiety (sal-MOF) was synthesized and postsynthetically metalated with iron and cobalt salts to afford robust and highly active single-site solid catalysts for olefin hydrogenation.

sal-MOF was constructed from the dicarboxylate bridging ligand sal-TPD (Supporting Information (SI)) and the Zr-based secondary building unit (SBU) to afford a UiO framework of Zr$_6$O$_4$(OH)$_4$(sal-TPD)$_6$.[47] UiO-type MOFs have been used for many catalytic reactions owing to their excellent stability.[46,48]

sal-MOF was synthesized by heating ZrCl$_4$ and H$_2$sal-TPD in a DMF solution in the presence of trifluoroacetic acid. Single-crystal X-ray diffraction studies revealed a UiO-type structure for sal-MOF, which crystallizes in the $Fm\bar{3}m$ space group and contains both octahedral and tetrahedral cages with edges measuring 15 Å. As the sal groups could not be accurately located on the electron density map due to partial decomposition of H$_2$sal-TPD during MOF synthesis and crystallographic disorder of the side chains, the presence of the sal moiety in the MOF was instead established and quantified by ^{1}H NMR spectra of digested MOF samples. NMR studies consistently revealed that ∼80% of the sal moiety remains intact in the sal-MOF under the synthesis conditions (Figure S4, SI). The powder X-ray diffraction (PXRD) pattern of sal-MOF is identical with the pattern simulated from the single-crystal structure (Figure 1d). Nitrogen sorption measurements indicate that sal-MOF is highly porous with a BET surface area of 3311 m^2/g and pore sizes of 8.2 and 11.1 Å (Figure 1b and Figure S10, SI).

Postsynthetic metalation was performed by treating sal-MOF with 5.0 equiv of FeCl$_2$·4H$_2$O in THF to afford sal-Fe-MOF as a brown solid or with 7.0 equiv of CoCl$_2$ in THF to afford sal-Co-MOF as a greenish blue solid. The crystallinity of sal-MOF was maintained upon metalation, as evidenced by similar PXRD patterns of sal-MOF and sal-M-MOFs (Figure 1d,e). Inductively coupled plasma-mass spectrometry (ICP-MS) analyses of the digested metalated MOFs provided Fe and Co loadings of 66%
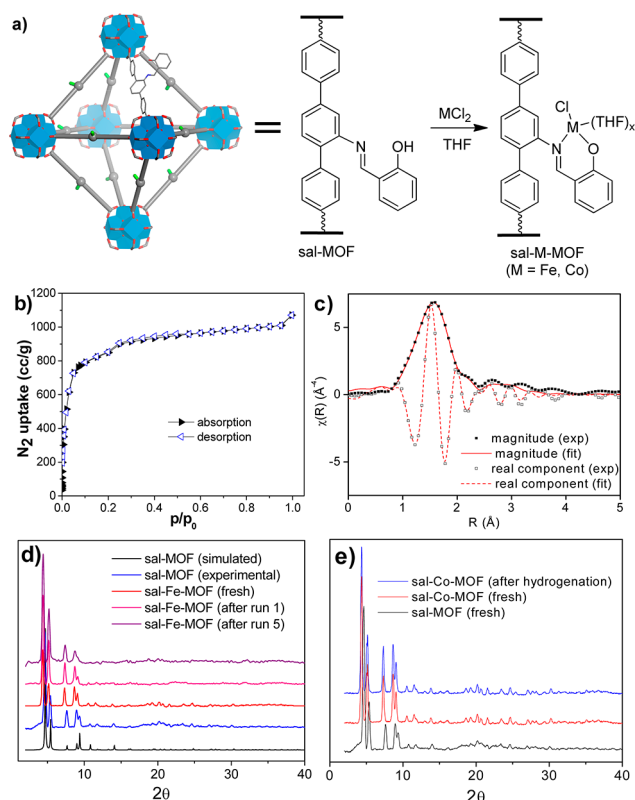
Figure 1. (a) Postsynthetic metalation of sal-MOF to form sal-M-MOFs. (b) Nitrogen sorption isotherm of sal-MOF. (c) Experimental EXAFS spectra at the Fe K edge of sal-Fe-MOF and fits in R space showing the magnitude (solid squares, solid line) and real component (hollow squares, dash line) of the Fourier transform. (d) PXRD pattern simulated from the CIF file (black) and PXRD patterns of pristine sal-MOF (blue), freshly prepared sal-Fe-MOF (red), and sal-Fe-MOF recovered from the first (pink) and fifth runs (purple) of 1-octene hydrogenation. (e) PXRD patterns of pristine sal-MOF (black), freshly prepared sal-Co-MOF (red), and sal-Co-MOF recovered from hydrogenation of 1-octene (blue).

and 6% for sal-Fe-MOF and sal-Co-MOF, respectively. The Co loading increased to 80% when the MOF was first treated with t-BuOK. ^{1}H NMR spectra of digested sal-Fe and sal-Co MOFs showed that the sal moiety remained intact within the MOFs upon metalation. sal-Fe-MOF and sal-Co-MOF gave BET surface areas of 3101 and 3366 m^2/g, respectively, with pore size distributions remaining essentially unchanged from that of pristine sal-MOF (Figures S8−S10, SI). The surface area and pore aperture dimensions confirm the presence of open channels in the MOF, which suggests that the Fe and Co sites are accessible to alkenes during catalytic reactions.

Due to disorder as well as incomplete functionalization and metalation of the sal-MOF, the Fe coordination environment in sal-Fe-MOF cannot be studied by X-ray crystallography. Instead, we performed X-ray absorption spectroscopy (XAS) at the Fe K edge to investigate the Fe coordination environment. A model of the precatalyst was generated on the basis of the single-crystal structures of $Fe_4(sal)_4Cl_4(THF)_2$ (Figure 2a) and $Fe(t$-Busal$)_2$.[49] Fitting the extended X-ray absorption fine structure (EXAFS) region of the XAS spectrum with the structure model reveals a Fe(II) complex containing the sal moiety, one chloride, and two to three THF solvent molecules as ligands (Figure 1c). DFT calculations suggest minimal energy differences (∼2.5 kcal/mol) between five- and six-coordinate Fe(II) structures (Figure 2b).
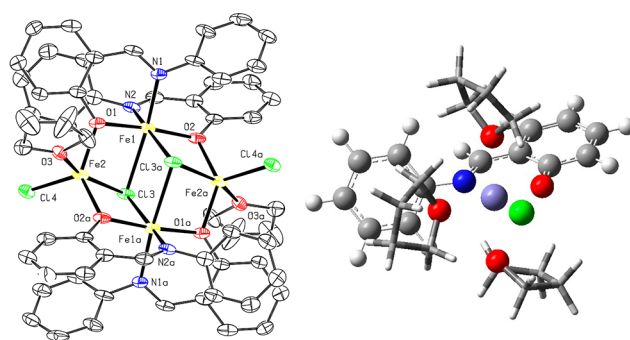

Figure 2. Crystal structure of $Fe_4(sal)_4Cl_4(THF)_2$ (left) and DFT calculated structure of $Fe(sal)Cl(THF)_3$ (right).

As EXAFS fits the average coordination environment for all Fe atoms in the sample, it is reasonable that the sample contains a mixture of five- and six-coordinate species, presumably due to the ease of losing coordinated THF molecules during sample handling.

Conditions for hydrogenation were optimized by treating sal-Fe-MOF with several hydride reagents. Upon treatment with NaEt$_3$BH in THF, sal-Fe-MOF is a highly active catalyst for hydrogenation of olefins. Treatment of 0.01 mol % of sal-Fe-MOF with NaBEt$_3$H (8 equiv with respect to Fe) in THF for 1 h followed by washing with THF led to a highly active hydrogenation catalyst that completely converted 1-octene to n-octane under 40 atm of H$_2$ in 18 h. The rate of hydrogenation was unchanged in the presence of mercury (Table 1, entry 6),

Table 1. Optimization of Reaction Conditions for sal-Fe-MOF-Catalyzed Hydrogenation of 1-Octene[a]

entry	cat. treatment	solvent	time (h)	yield (%)
1	NaBEt$_3$H	THF	16	100
2	n-BuLi	THF	18	0
3	EtMgCl	THF	18	0
4	Et$_2$Zn	THF	18	0
5	NaBEt$_3$H	THF	16	100[b]
6	NaBEt$_3$H/Hg[c]	THF	16	100[b]
7	NaBEt$_3$H	toluene	16	92[b]

[a]Reaction conditions: 3.0 mg of sal-Fe-MOF (0.1 mol % Fe), 0.8 mol % of cat. treatment, 1.56 mmol of 1-octene, 0.5 mL of solvent. [b]0.01 mol % of Fe. [c]One drop of Hg was added before adding 1-octene.

which suggests that in situ generated Fe nanoparticles were not responsible for the observed catalysis and that Fe—hydride is the active species. Additionally, sal-Fe-MOF displayed higher catalytic activity in THF in comparison to that in methylene chloride and hydrocarbon solvents. Impressively, under the optimized reaction conditions, sal-Fe-MOF gave a turnover number (TON) of 1.45×10^5 for the hydrogenation of 1-octene (Table 2, entry 2).

sal-Fe-MOF displayed excellent activity in the hydrogenation of a wide range of aliphatic and aromatic terminal alkenes (Table 2). At 0.05−0.01 mol % catalyst loading, styrene and its alkoxy and halide derivatives were hydrogenated with complete conversion, affording the corresponding products in 93−100% yield (Table 2, entries 4, 7, and 8). sal-Fe-MOF also displayed high TONs and excellent yields for the hydrogenation of gem-disubstituted alkenes, such as α-methylstyrene, and dialkenes

Table 2. sal-M-MOF-Catalyzed Hydrogenation of Olefins[a]

$$R_2R_1C{=}CR_3 \xrightarrow[\text{THF, 23 °C}]{\substack{\text{sal-M-MOF} \\ \text{40 atm } H_2}} R_2R_1CH{-}CH_2R_3$$

Entry	Substrate	M	Time	% Yield	TON
1	(n-hexenyl)	Fe	18 h	100	10000
2			8 d	94	145000[b]
3		Co	18 h	75	25000
4	C_6H_5-CH=CH$_2$	Fe	18 h	100	10000
5			24 h	44	44000[c]
6		Co	18 h	55	18300
7	4-FC$_6$H$_4$-CH=CH$_2$	Fe	48 h	100	>20000[d]
8	4-MeOC$_6$H$_4$-CH=CH$_2$	Fe	24 h	100	>10000
9		Co	18 h	100	>2000[e]
10	C_6H_5-C(CH$_3$)=CH$_2$	Fe	18 h	100	>10000
11		Co	18 h	100	>2000[e]
12	(diene)	Fe	24 h	100	>2000[e]
13		Co	18 h	100	>2000[e]
14	(diallyl ether)	Fe	24 h	100	>1000[f]
15	(cyclohexene)	Fe	18 h	100	>1000[f]
16		Co	18 h	100	>2000[e]
17	C_6H_5-CH=CH-CH$_3$	Fe	70 h	36	360[f]
18	MeOOC-C(=CH$_2$)-CH$_2$-COOMe	Fe	24 h	62	620[f]
19	allyl acetate	Fe	70 h	64	640[f]
20		Co	72 h	0	0[e]
21	methylacrylaldehyde	Fe	3 d	76	760[f]

[a]Reaction conditions: 0.01 mol % of sal-Fe-MOF or 0.003 mol % of sal-Co-MOF, 10 equiv of NaBEt$_3$H (1.0 M in THF), alkene, THF, 40 atm of H$_2$, 23 °C. [b]6.5 × 10^{-4} mol % of catalyst. [c]0.001 mol % of catalyst. [d]0.005 mol % of catalyst. [e]0.05 mol % of catalyst. [f]0.1 mol % of catalyst.
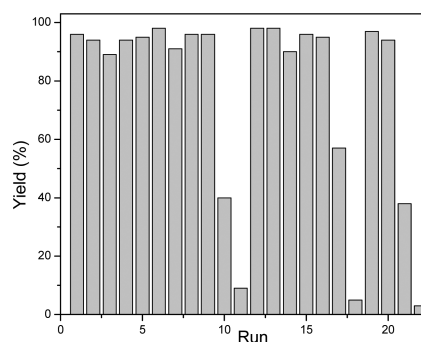

Figure 3. Plot of yield (%) of n-octane at various runs in the recycle and reuse of sal-Fe-MOF (0.5 mol % Fe) for hydrogenation of 1-octene. sal-Fe-MOF was regenerated after runs 11 and 18 by treating with NaBEt$_3$H in THF.

such as 1,7-octadiene and allyl ether (Table 2, entries 10, 12, and 14). Although the internal olefin cyclohexene was readily hydrogenated, cis-β-methylstyrene required longer reaction times. sal-Fe-MOF is tolerant of aldehyde, ketone, and ester functional groups. Functionalized alkenes such as dimethyl itaconate, allyl acetate, and methylacrylaldehyde were selectively reduced to dimethyl 2-methylsuccinate, propyl acetate, and isobutyraldehyde, respectively (Table 2, entries 18, 19, and 21).

Remarkably, at a 0.5 mol % catalyst loading, sal-Fe-MOF could be recovered and reused for 1-octene hydrogenation at least eight times without loss of catalytic activity (Figure 3) or MOF crystallinity (Figure 1d). Excellent yields (89−99%) of n-octane were obtained consistently in the reuse experiments with no observation of alkene isomerization or other byproducts. The catalytic activity of sal-Fe-MOF dropped significantly after run 9, and poor conversion of 1-octene was observed at run 11 even after a longer reaction time (Figure 3). Interestingly, the catalyst could be regenerated by simply treating with 10 equiv of NaBEt$_3$H followed by washing with THF. The regenerated MOF

catalyst could be recovered and reused another six times before further deactivation. The decrease in activity could be attributed to multiple factors, including cumulative iron site deactivation by trace amounts of air or water and diminished MOF crystallinity following repeated recycling and reuse experiments. The heterogeneity of sal-Fe-MOF was confirmed by several experiments. The PXRD patterns of sal-Fe-MOF recovered from the first and fifth runs remained unchanged from that of pristine sal-Fe-MOF (Figure 1d), indicating the stability of the MOF framework under the catalytic conditions. Additionally, ICP-MS analyses showed that the amounts of Fe and Zr leaching into the supernatant after the first run were 0.074 and 0.004%, respectively and after the fourth run were 0.069% and 0.003%, respectively. Moreover, no further hydrogenation was observed after removal of sal-Fe-MOF from the reaction mixture (Scheme S3, SI). An additional control experiment was performed with only FeCl$_2$ and NaBEt$_3$H at a loading equivalent to the amount of iron leached from the MOF. No conversion was observed by NMR spectroscopy, showing that the leached iron species is not responsible for the catalytic activity.

sal-Co-MOF is also active in olefin hydrogenation upon treatment with 8 equiv of NaBEt$_3$H in THF. At 0.05 mol % Co loading, several aliphatic and aromatic alkenes, including dienes and internal olefins, were hydrogenated with full conversion (Table 2, entries 3, 6, 9, 11, 13, and 17). A maximum TON of 25000 was observed for sal-MOF-Co with 1-octene as the substrate. The sal-Co-MOF recovered from the dehydrogenation showed the same PXRD pattern as the pristine sal-MOF (Figure 1e), indicating that the sal-Co-MOF framework is also stable under the catalytic conditions.

We also prepared molecular (sal)Fe(THF)$_x$Cl species in order to investigate the role of the framework in stabilizing the sal-M catalysts. Repeated synthetic attempts under a variety of conditions afforded a tetrameric species with the formula of Fe$_4$(sal)$_4$Cl$_4$(THF)$_2$, as revealed by single-crystal X-ray diffraction (Figure 2a). Formation of such a tetranuclear complex is expected, as low-coordination-number Fe species are not stable in solution and can oligomerize through Cl or O bridging ligands. In contrast, oligomerization is prohibited in sal-M-MOFs due to isolation of the metal sites. Importantly, Fe$_4$(sal)$_4$Cl$_4$(THF)$_2$ was inactive toward olefin hydrogenation following the same treatment with 8 equiv of NaBEt$_3$H, revealing the critical role of site isolation for stabilizing low-coordinate sal-M catalysts.

In summary, we have developed a novel postsynthetic metalation strategy to discover MOF-supported base-metal catalysts which do not possess homogeneous counterparts. UiO

MOFs bearing the M−salicylaldimine moiety (M = Fe, Co) are highly active single-site solid catalysts for alkene hydrogenation and can be readily recycled and reused. This work thus shows that MOFs provide a new platform for discovering base-metal catalysts with potential application in the practical synthesis of fine chemicals.

■ ASSOCIATED CONTENT

Ⓢ Supporting Information

Text, figures, tables, and CIF files giving general experimental details, synthesis and characterization of the ligand and MOFs, MOF-catalyzed hydrogenation reactions, MOF catalyst recycle and reuse procedures, EXAFS details and fits, DFT calculation details, and crystallographic data. This material is available free of charge via the Internet at http://pubs.acs.org.

■ AUTHOR INFORMATION

Corresponding Author
E-mail for W.L.: wenbinlin@uchicago.edu.

Author Contributions
[†]These authors contributed equally.

Notes
The authors declare no competing financial interest.

■ ACKNOWLEDGMENTS

■ REFERENCES

(1) Johnson Matthey. *Platinum Today*; www.platinum.matthey.com.
(2) Bolm, C.; Legros, J.; Le Paih, J.; Zani, L. *Chem. Rev.* **2004**, *104*, 6217.
(3) Enthaler, S.; Junge, K.; Beller, M. *Angew. Chem., Int. Ed.* **2008**, *47*, 3317.
(4) Sun, C.-L.; Li, B.-J.; Shi, Z.-J. *Chem. Rev.* **2010**, *111*, 1293.
(5) Nakazawa, H.; Itazaki, M.; Plietker, B. *Top. Organomet. Chem.* **2011**, *33*, 27.
(6) Gephart, R. T.; Warren, T. H. *Organometallics* **2012**, *31*, 7728.
(7) Friedfeld, M. R.; Shevlin, M.; Hoyt, J. M.; Krska, S. W.; Tudge, M. T.; Chirik, P. J. *Science* **2013**, *342*, 1076.
(8) Hennessy, E. T.; Betley, T. A. *Science* **2013**, *340*, 591.
(9) Chen, C.; Dugan, T. R.; Brennessel, W. W.; Weix, D. J.; Holland, P. L. *J. Am. Chem. Soc.* **2014**, *136*, 945.
(10) de Vries, J. G.; Elsevier, C. J. *Handbook of Homogeneous Hydrogenation*; Wiley-VCH: Weinheim, Germany, 2007.
(11) Bart, S. C.; Lobkovsky, E.; Chirik, P. J. *J. Am. Chem. Soc.* **2004**, *126*, 13794.
(12) Casey, C. P.; Guan, H. *J. Am. Chem. Soc.* **2007**, *129*, 5816.
(13) Sui-Seng, C.; Freutel, F.; Lough, A. J.; Morris, R. H. *Angew. Chem., Int. Ed.* **2008**, *47*, 940.
(14) Mikhailine, A.; Lough, A. J.; Morris, R. H. *J. Am. Chem. Soc.* **2009**, *131*, 1394.
(15) Morris, R. H. *Chem. Soc. Rev.* **2009**, *38*, 2282.
(16) Federsel, C.; Boddien, A.; Jackstell, R.; Jennerjahn, R.; Dyson, P. J.; Scopelliti, R.; Laurenczy, G.; Beller, M. *Angew. Chem., Int. Ed.* **2010**, *49*, 9777.
(17) Enthaler, S.; Haberberger, M.; Irran, E. *Chem. Asian J.* **2011**, *6*, 1613.
(18) Haberberger, M.; Irran, E.; Enthaler, S. *Eur. J. Inorg. Chem.* **2011**, *2011*, 2797.
(19) Zuo, W.; Lough, A. J.; Li, Y. F.; Morris, R. H. *Science* **2013**, *342*, 1080.
(20) Morys, P.; Schlieper, T. *J. Mol. Catal. A: Chem.* **1995**, *95*, 27.
(21) Zhang, X.; Geng, Y.; Han, B.; Ying, M.-Y.; Huang, M.-Y.; Jiang, Y.-Y. *Polym. Adv. Technol.* **2001**, *12*, 642.
(22) Phua, P.-H.; Lefort, L.; Boogers, J. A. F.; Tristany, M.; de Vries, J. G. *Chem. Commun.* **2009**, 3747.
(23) Stein, M.; Wieland, J.; Steurer, P.; Tölle, F.; Mülhaupt, R.; Breit, B. *Adv. Synth. Catal.* **2011**, *353*, 523.
(24) Iablokov, V.; Beaumont, S. K.; Alayoglu, S.; Pushkarev, V. V.; Specht, C.; Gao, J.; Alivisatos, A. P.; Kruse, N.; Somorjai, G. A. *Nano Lett.* **2012**, *12*, 3091.
(25) Welther, A.; Bauer, M.; Mayer, M.; Jacobi von Wangelin, A. *ChemCatChem* **2012**, *4*, 1088.
(26) Hudson, R.; Hamasaka, G.; Osako, T.; Yamada, Y. M. A.; Li, C.-J.; Uozumi, Y.; Moores, A. *Green Chem.* **2013**, *15*, 2141.
(27) Kelsen, V.; Wendt, B.; Werkmeister, S.; Junge, K.; Beller, M.; Chaudret, B. *Chem. Commun.* **2013**, *49*, 3416.
(28) Mokhov, V. M.; Popov, Y. V.; Nebykov, D. N. *Russ. J. Gen. Chem.* **2014**, *84*, 622.
(29) Jagadeesh, R. V.; Surkus, A.-E.; Junge, H.; Pohl, M.-M.; Radnik, J.; Rabeah, J.; Huan, H.; Schünemann, V.; Brückner, A.; Beller, M. *Science* **2013**, *342*, 1073.
(30) Li, H.; Eddaoudi, M.; O'Keeffe, M.; Yaghi, O. M. *Nature* **1999**, *402*, 276.
(31) Moulton, B.; Zaworotko, M. J. *Chem. Rev.* **2001**, *101*, 1629.
(32) Kitagawa, S.; Kitaura, R.; Noro, S.-i. *Angew. Chem., Int. Ed.* **2004**, *43*, 2334.
(33) Das, M. C.; Xiang, S.; Zhang, Z.; Chen, B. *Angew. Chem., Int. Ed.* **2011**, *50*, 10510.
(34) Della Rocca, J.; Liu, D.; Lin, W. *Acc. Chem. Res.* **2011**, *44*, 957.
(35) Horcajada, P.; Gref, R.; Baati, T.; Allan, P. K.; Maurin, G.; Couvreur, P.; Férey, G.; Morris, R. E.; Serre, C. *Chem. Rev.* **2012**, *112*, 1232.
(36) Suh, M. P.; Park, H. J.; Prasad, T. K.; Lim, D.-W. *Chem. Rev.* **2012**, *112*, 782.
(37) Sumida, K.; Rogow, D. L.; Mason, J. A.; McDonald, T. M.; Bloch, E. D.; Herm, Z. R.; Bae, T.-H.; Long, J. R. *Chem. Rev.* **2012**, *112*, 724.
(38) Yoon, M.; Srirambalaji, R.; Kim, K. *Chem. Rev.* **2012**, *112*, 1196.
(39) Wang, C.; Liu, D.; Lin, W. *J. Am. Chem. Soc.* **2013**, *135*, 13222.
(40) Lee, J.; Farha, O. K.; Roberts, J.; Scheidt, K. A.; Nguyen, S. T.; Hupp, J. T. *Chem. Soc. Rev.* **2009**, *38*, 1450.
(41) Ma, L.; Abney, C.; Lin, W. *Chem. Soc. Rev.* **2009**, *38*, 1248.
(42) Zhang, X.; Llabrés i Xamena, F. X.; Corma, A. *J. Catal.* **2009**, *265*, 155.
(43) Ma, L.; Falkowski, J. M.; Abney, C.; Lin, W. *Nat. Chem.* **2010**, *2*, 838.
(44) Song, F.; Wang, C.; Falkowski, J. M.; Ma, L.; Lin, W. *J. Am. Chem. Soc.* **2010**, *132*, 15390.
(45) Wang, C.; Wang, J.-L.; Lin, W. *J. Am. Chem. Soc.* **2012**, *134*, 19895.
(46) Manna, K.; Zhang, T.; Lin, W. *J. Am. Chem. Soc.* **2014**, *136*, 6566.
(47) Cavka, J. H.; Jakobsen, S.; Olsbye, U.; Guillou, N.; Lamberti, C.; Bordiga, S.; Lillerud, K. P. *J. Am. Chem. Soc.* **2008**, *130*, 13850.
(48) Falkowski, J. M.; Sawano, T.; Zhang, T.; Tsun, G.; Chen, Y.; Lockard, J. V.; Lin, W. *J. Am. Chem. Soc.* **2014**, *136*, 5213.
(49) Becker, J. M.; Barker, J.; Clarkson, G. J.; van Gorkum, R.; Johal, G. K.; Walton, R. I.; Scott, P. *Dalton Trans.* **2010**, *39*, 2309.